Proceedings of the 28th IEEE
EMBS Annual International Conference
New York City, USA, Aug 30-Sept 3, 2006

The role of flexible polymer interconnects in chronic tissue response induced by intracortical microelectrodes – a modeling and an *in vivo* study

Jeyakumar Subbaroyan and Daryl R. Kipke, Member, *IEEE*

Abstract – Chronic tissue response induced by tethering is one of the major causes for implant failure in intracortical microelectrodes. In this study, we had explored the hypothesis that flexible interconnects could provide strain relief against forces of "micromotion" and hence could result in maintaining a healthy tissue surrounding the implant. Finite element modeling results indicated that flexible interconnects, namely polyimide (E = 2 GPa) and polydimethylsiloxane (PDMS, E = 6 MPa), reduced the interfacial strain by 66% and two orders of magnitude, respectively. Quantitative immunohistochemistry results indicated that significant neuronal loss occurred up to 60 μm from the implant interface. This was strongly correlated to both glial fibrillary acidic protein (GFAP) expression and simulated strain as a function of distance away from the implant.

I. Introduction

Loss of recording capabilities of a chronic intracortical microelectrode could be caused by a severe chronic tissue response leading up to extensive neuronal loss in the effective recording distance (defined as 80 μm to 130 μm around the implant). Electrical and chemical intervention strategies could be used to improve this condition post-implant [1-4]. A different approach involves modifying the mechanical properties of the implant material. In this study, we have simulated the strain induced by an intracortical microelectrode with a flexible interconnect on the tissue surrounding the implant using a 3-D finite element model (FEM). "Micromotion" – defined as relative movement of implant with respect to tissue – is believed to induce the strain. The model results have been correlated to quantitative immunohistochemical results.

II. Methods

A. Finite element modeling

A 3-D FEM of the electrode-tissue interface was developed in ABAQUS 6.4 (ABAQUS, Inc., RI) to simulate interfacial strain caused by implant micromotion (Figure 1). Details of the model are described elsewhere [5]. Our previous work had simulated the effect of substrate stiffness and electrode-tissue adhesion on the strain induced in the tissue. In the current work, the effect of interconnect stiffness on the interfacial strain was simulated. Three materials, silicon (E = 200 GPa), polyimide (E = 2 GPa) and poly dimethyl siloxane (PDMS, E = 6 MPa), were simulated. In all three cases, an interconnect of finite length and radius of curvature was used while the implanted shank material simulated was silicon. Boundary conditions were applied such that the base of the brain tissue (edges AB and BC) was fixed throughout the simulations. A displacement of 1 μm was applied to the end of interconnect to simulate micromotion. The resulting maximum principal strain was plotted as a function of distance from the interface at the tip, mid-point and surface of the probe tract in the brain tissue.

B. Polymer cable microfabrication

Polydimethylsiloxane (PDMS) cables were batch fabricated using microelectronic process techniques in a class 10,000 cleanroom. Briefly, a 100 nm sacrificial aluminum layer was e-beam evaporated onto a 4 inch silicon wafer. A 100 μm layer of SU-8 2075 (Microchem Corp., MA), a negative, epoxy based photoresist was spun onto the wafer. The SU-8 layer acts as the mold for PDMS cables. Photoresist was exposed, developed and hard baked. PDMS was prepared by mixing pre-polymer with curing agent in a 10:1 ratio. The mixture was spun and the excess polymer was scrapped off using a razor blade. The wafer was baked at 150 C for 12 hours. Residual PDMS was etched away in CF4/O2 plasma (3:1) for a few seconds. Finally, SU-8 molds were released in KOH etch. PDMS cables were then peeled off using a pair of tweezers.

C. Chamber machining and assembly

To test our hypothesis on flexibility of interconnects, the implant had to be suspended freely above the cortical surface thus allowing for "micromotion" of the implant. This was achieved by suspending the interconnect in a fluidic chamber. The chamber was 4 mm tall and had a foot print of 12 mm. There was a 5 mm X 3 mm rectangular opening at the base for craniotomy. After machining, the chamber was sterilized by soaking in 70% ethanol for 5 minutes. A 5 μm layer of parylene-c, a biocompatible polymer, was deposited onto the chamber.

Device assembly was carried out in a class 100,000 cleanroom. Using a sterile surgical scalpel, interconnect of a single shank Michigan silicon probe was fractured. PDMS cable, with exact width and length as the original interconnect, was glued onto the silicon front end using medical grade silicone (MED-4211, NuSil Technology LLC, CA). The assembled device was cured at 100 C for 15 minutes. The device was then glued onto the chamber using

Manuscript received April 24, 2006. This work was supported in part by grants from NIH/NIBIB (P41 EB-00230-10). The Engineering Research Centers program of the National Science Foundation (EEC-9986866) and NASA Biosciences and Engineering Institute (NNCO4AA21A).

J. Subbaroyan and D. R. Kipke are with the Biomedical Engineering Department, University of Michigan, Ann Arbor, MI 48109, USA (email: sjkumar@umich.edu; dkipke@umich.edu)

medical grade silicone. The assembly was left to cure at room temperature overnight under a sterile flow hood. Figure 2 shows an assembled chamber.

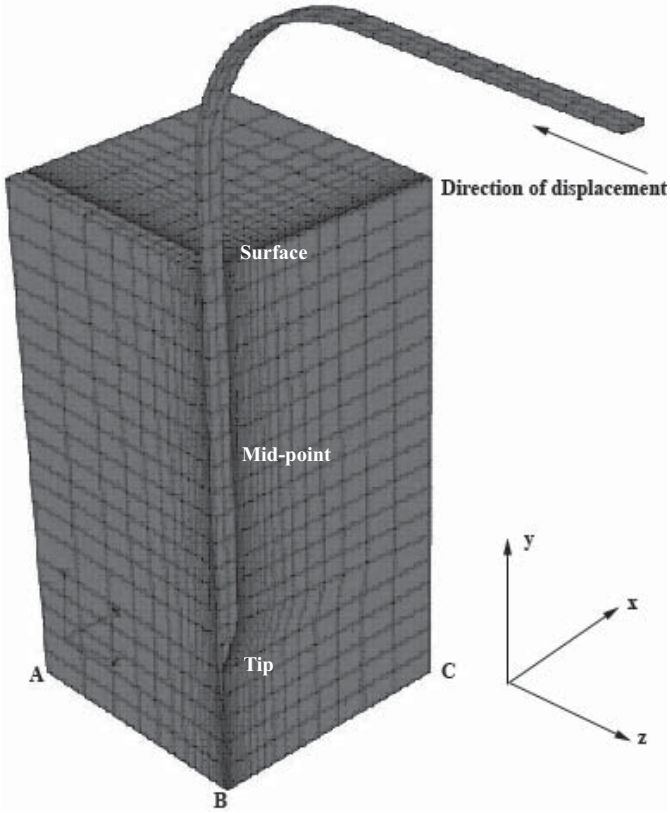

Figure 1. 3-D model of the electrode-tissue interface with the interconnect extending above the surface of the brain tissue. Edges AB and BC were fixed while a small displacement was applied to the end of the interconnect.

D. Surgical procedure

Three adult, male Sprague-Dawley (300-350g) rats were implanted with the chamber. Animals were anesthetized with a mixture of ketamine, xylazine and acepromazine. Animals' head were shaved, sterilized using betadiene and 70% ethanol and mounted onto a stereotaxic frame. A 5 mm x 3 mm craniotomy was made, centered over the primary motor cortex. Dura was resected and peeled back. Liberal application of sterile saline ensured that the brain was kept moist throughout the procedure. A bone scrapper was used to roughen the surface surrounding the craniotomy. Kwik-Sil (WPI, Inc., FL) was applied around the craniotomy and on the base of the chamber. The chamber was mounted on the skull such that the rectangular opening at its base lined up with the craniotomy. Care was taken to ensure that the silicone did not drip into the craniotomy. Once cured, the chamber was tested for leaks. Using a pair of sterile surgical microforceps, the probe was implanted in the brain tissue.

E. Perfusion and tissue processing

All animals were sacrificed through transcardial perfusion at the 4 week time point. Tissue was fixed by applying 100mL of sterile saline followed by 600 mL of 4% (w/v) paraformaldehyde. Brain tissue was immediately explanted and postfixed overnight in 4% (w/v) paraformaldehyde. This was followed by rinsing the tissue twice in 1X PBS and equilibration in 30% sucrose in PBS. The tissue was then sectioned at 12-µm thickness on a cryostat.

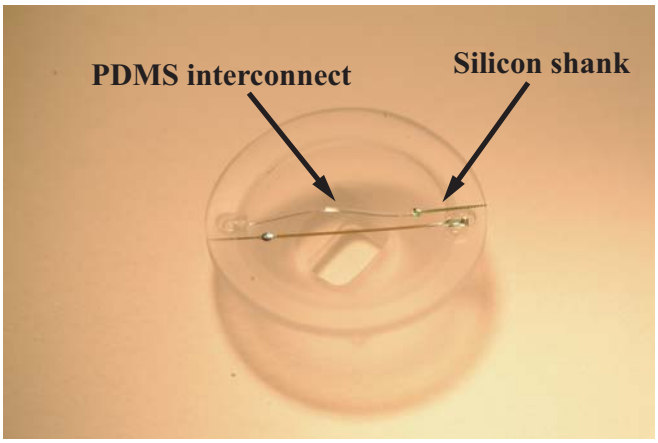

Figure 2. A plexiglass fluidic chamber assembled with a flexible PDMS interconnect and a "stiff" silicon implantable portion. The base of the chamber has a 5mm x 3mm opening for craniotomy.

F. Immunohistochemistry

Six tissue sections between cerebral cortex layers II and V were randomly selected to be immunostained. All antibodies were diluted in blocking solution consisting of 10% normal goat serum and 0.3% Triton-X 100. Sections were treated with blocking solution for 1 hour at room temperature. This was followed by overnight application of primary antibodies (NeuN 1:1000 and GFAP 1:400). Alexa Fluor 488 and Alexa Fluor 568 (Invitrogen Corporation, CA) were diluted in a blocking solution to a concentration of 5 µg/mL and applied for 2 hours at room temperature. Sections were counterstained with 2 µg/mL of 4', 6-Diamidino-2-phenylindole (DAPI). Tissue sections were mounted with a coverglass using Prolong Gold antifade reagent (Invitrogen Corporation, CA).

G. Imaging and quantification

Images were captured using Olympus BX-51 optical microscope at sub-saturating exposure for each specimen. Void left by probe explantation was centered in the image field. The same exposure time was used to capture the control image at approximately the same co-ordinates on the contralateral hemisphere. A differential interference contrast (DIC) image was used to define the probe-tissue boundary for all quantification steps. A pixel extraction algorithm using line profiling (n=208) was developed in Matlab (The Mathworks, Inc., MA) to obtain GFAP fluorescent intensity values. With the aid of a Matlab application, a blinded subject performed NeuN+ cell counting for up to 100 µm

from the electrode-tissue interface and the results were grouped in 20 μm bins.

III. Results

A. Interfacial strain

Maximum principal strain was plotted for different interconnect materials as a function of distance from the electrode-tissue interface at the surface, mid-point and the tip of the probe tract in the tissue (Figure 3). For all interconnect materials, the strain dropped off exponentially away from the interface. Maximum strain occurred at the tip of the probe tract for a silicon interconnect. All strain values were normalized with respect to this value. Two distinct features of the results were changes in the magnitude and the location of the strain. While a polyimide interconnect caused a 66% decrease in the maximum strain compared to its silicon counterpart, an ultra-flexible interconnect like PDMS resulted in two orders of magnitude smaller value of strain. Using a flexible interconnect focused the strain on the superficial layers of the brain tissue.

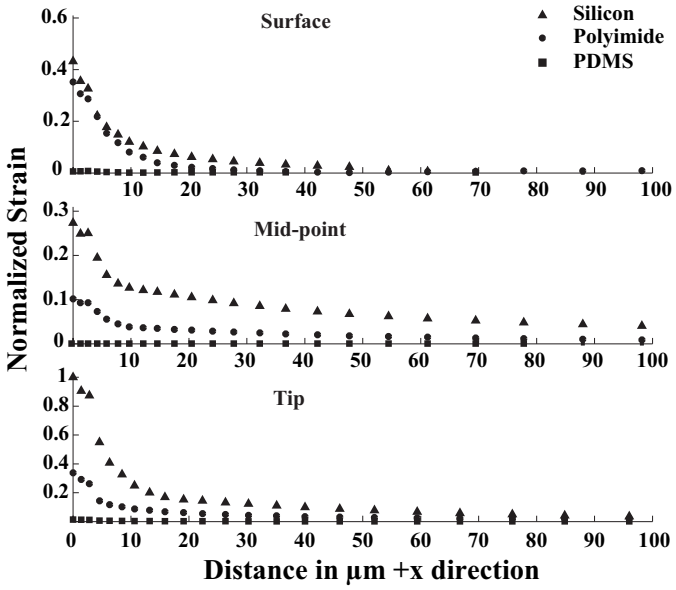

Figure 3. Normalized strain plotted as a function of distance in +x direction at three different locations – surface, mid-point and tip. The strain values decreased exponentially as a function of distance away from the interface.

B. GFAP expression and scar tissue formation

GFAP was significantly upregulated around the implant site at the 4 week time point. The relative fluorescent intensity dropped off exponentially as a function of distance from the interface (Figure 4). Astrocytic morphology was hypertrophied while GFAP up regulation was limited to about 250 μm from the interface. Astrocytic processes formed end feet engulfing the probe tract with a thin layer of loosely packed DAPI+/GFAP- layer sandwiched in between. In some cases, this layer was tightly packed and extended up to a few tens of microns from the interface. Previously published works report this layer to be activated microglia or macrophages of fibroblastic origin [6]. The fibrotic scar did not occur symmetrically around the probe tract. DAPI+/GFAP- region was also NeuN-.

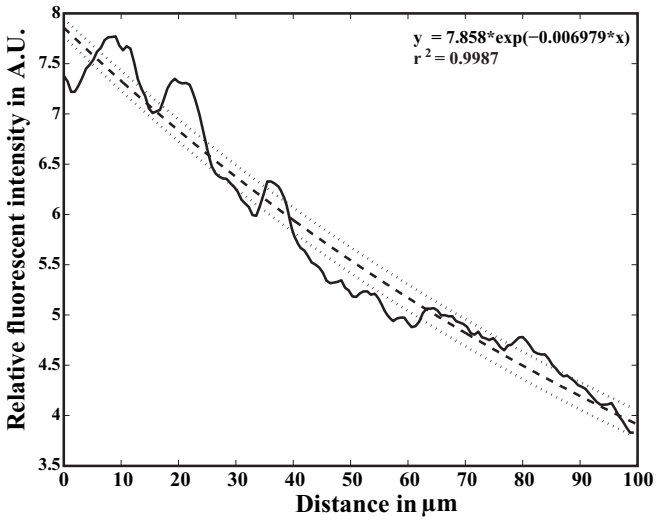

Figure 4. Relative GFAP intensity falls off exponentially as a function of distance from the interface (solid line). The broken line is the fitted curve while dotted lines are 95% confidence intervals.

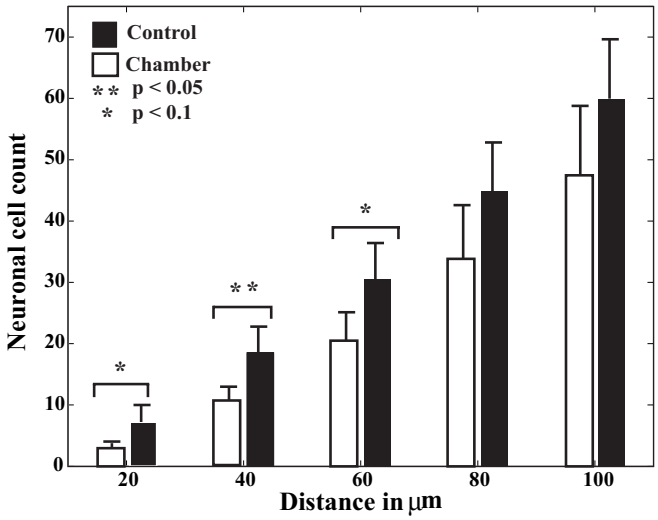

Figure 5. Neuronal cell count as a function of distance from the interface. There was significant loss of NeuN+ cells in the first 60 μm around the interface compared to healthy, contralateral tissue.

C. Neuronal density around the interface

$NeuN^+$ cells were counted and grouped into 20 μm bins. There was a 21±11% decrease in neuronal cell count in the first 100 μm from the electrode-tissue interface. The loss was significant up to 60 μm from the interface (Figure 5). Normalized neuronal loss decreased exponentially as a function of distance from the interface.

IV. Discussion

Empirical evidence suggests that tethering forces alone cause extensive damage in the vicinity of the implant [7]. We therefore believe that by modifying those forces and limiting the extent of "micromotion", a healthy, near normal interface could be maintained around an intracortical microelectrode. One approach to achieve this is to modify the mechanical properties of the implant, namely substrate stiffness and interconnect stiffness.

The effect of substrate stiffness and tissue adhesion properties on the interfacial strains around an intracortical microelectrode were simulated in our previous work [5]. However, implanting a flexible substrate into brain tissue poses several problems including fabrication and insertion. Hence, in the current work, we had explored the possibility of using flexible interconnects to provide strain relief against tethering forces causing "micromotion".

The results of FEM simulations indicated that flexible interconnects caused smaller strain values in the tissue compared to their stiff counterpart, silicon. A polyimide interconnect (100 times more flexible than silicon) caused 66% smaller strain while a PDMS interconnect (~ 33,000 times more flexible than silicon) caused two orders of magnitude smaller strain. These polymers, when used as substrate materials, resulted in 94% and two orders of magnitude decrease in strain values, respectively [5]. The maximum strain was focused at the surface and superficial layers of the brain tissue when a flexible interconnect was used whereas a stiff interconnect caused elevated strain at the tip. These observations are similar to our previously reported results [5]. The results indicate that reducing interconnect stiffness could reduce interfacial strain thereby reducing shear induced damages around the implant. Also, by localizing strain at superficial layers of the brain tissue (Layer I and II), which are of little interest to neural prosthesis, flexible interconnects provide a healthy neuronal interface to record from or stimulate in the deeper cortical structures (Layer V).

The strain induced is also a function of interconnect length since any micromotion induced displacement shall be amplified by the length and hence translate into higher strains at the interface. The radius of curvature or the angle of cable bending also affects the strain distribution. A probe used in the simulations with a silicon cable length of 1 cm could result in a uniformly distributed (static) force of 6.25 μN along the length of the shank while this force is negligible for a polyimide or a PDMS cable. While these factors had been taken into consideration while developing the model, simulations were not performed to estimate the extent of their influence on the interfacial strain.

GFAP up regulation and neuronal loss are indicators of traumatic brain injury and the subsequent healing of the brain tissue. Both dropped off exponentially as a function of distance away from the interface. Normalized neuronal loss was strongly correlated with GFAP expression in the 100 μm surrounding the interface (Correlation co-efficient = 0.9930, p-value = 7×10^{-4}). They also correlated to the interfacial strain simulated by the model (Correlation co-efficient = 0.9004, p-value = 0.0371). These results suggest that a cause/effect relationship could possibly exist between mechanical strain around the interface caused by micromotion and its general wellbeing.

Experiments are in progress to test the effect of three different tethering forces on the tissue surrounding an implant. The study shall establish a gradation in tissue response as a function of interconnect flexibility. Once quantified, the immunohistochemistry metrics (GFAP expression, neuronal loss) shall be correlated to the results of the FEM.

V. Conclusion

A 3-D FEM of the electrode-tissue interface was developed and the effect of interconnect stiffness on the interfacial strain was simulated. An *in vivo* experiment to test the results of the model was carried out by implanting flexible polymer interconnect electrodes suspended in a fluidic chamber. Quantitative immunohistochemistry was used to assess implant performance in terms of GFAP expression and neuronal cell count. FEM results indicate that flexible polymer interconnects could cause a decrease in strain induced in the tissue by 66% (Polyimide) to two orders of magnitude (PDMS). Experimental results indicate significant neuronal loss up to 60 μm surrounding the implant. A strong correlation exists between simulated strain, GFAP expression and normalized neuronal loss in the 100 μm surrounding the implant.

Acknowledgment

The authors would like to thank Ted Webster and Dave Carter for machining the chamber, Keith Pennington for helpful hints on chamber design, Marta Dzaman for sectioning, Shelly Almburg for microscope training, Rita Kichenamourty for cell counting and John Seymour for helpful discussions on histology.

References

[1] Johnson, M.D., K.J. Otto, and D.R. Kipke, *Repeated voltage biasing improves unit recordings by reducing resistive tissue impedances.* IEEE Transactions on Neural Systems and Rehabilitation Engineering, 2005. **13**(2): p. 160-165.

[2] Retterer, S.T., et al., *Model neural prostheses with integrated microfluidics: A potential intervention strategy for controlling reactive cell and tissue responses.* IEEE Transactions on Biomedical Engineering, 2004. **51**(11): p. 2063-2073.

[3] Shain, W., et al., *Controlling cellular reactive responses around neural prosthetic devices using peripheral and local intervention strategies.* IEEE Transactions on Neural Systems and Rehabilitation Engineering, 2003. **11**(2): p. 186-188.

[4] Spataro, L., et al., *Dexamethasone treatment reduces astroglia responses to inserted neuroprosthetic devices in rat neocortex.* Experimental Neurology, 2005. **194**(2): p. 289-300.

[5] Subbaroyan, J., Martin, D.C., and Kipke, D.R., *A finite-element model of the mechanical effects of implantable microelectrodes in the cerebral cortex.* Journal of Neural Engineering, 2005. **2**: p. 103-113.

[6] Biran, R., D.C. Martin, and P.A. Tresco, *Neuronal cell loss accompanies the brain tissue response to chronically implanted silicon microelectrode arrays.* Experimental Neurology, 2005. **195**(1): p. 115-126.

[7] Kim, Y.T., et al., *Chronic response of adult rat brain tissue to implants anchored to the skull.* Biomaterials, 2004. **25**(12): p. 2229-2237.